SCIENTIFIC REPORTS

OPEN

SUBJECT AREAS:
HERPETOLOGY
ELECTRON MICROSCOPY
SPECTROPHOTOMETRY
NANOSCALE MATERIALS

Received
15 October 2012

Accepted
25 April 2013

Published
16 May 2013

Correspondence and requests for materials should be addressed to M.S. (spinner@uni-bonn.de)

# Snake velvet black: Hierarchical micro- and nanostructure enhances dark colouration in *Bitis rhinoceros*

Marlene Spinner[1,2], Alexander Kovalev[1], Stanislav N. Gorb[1] & Guido Westhoff[2,3]

[1]Functional Morphology and Biomechanics, Zoological Institute, Kiel University, Am Botanischen Garten 1–9, 24118 Kiel, Germany, [2]Institute of Zoology, University of Bonn, Poppelsdorfer Schloss, 53115 Bonn, Germany, [3]Tierpark Hagenbeck gGmbH, Lokstedter Grenzstr, Hamburg 22527, Germany.

**The West African Gaboon viper (*Bitis rhinoceros)* is a master of camouflage due to its colouration pattern. Its skin is geometrically patterned and features black spots that purport an exceptional spatial depth due to their velvety surface texture. Our study shades light on micromorphology, optical characteristics and principles behind such a velvet black appearance. We revealed a unique hierarchical pattern of leaf-like microstructures striated with nanoridges on the snake scales that coincides with the distribution of black colouration. Velvet black sites demonstrate four times lower reflectance and higher absorbance than other scales in the UV – near IR spectral range. The combination of surface structures impeding reflectance and absorbing dark pigments, deposited in the skin material, provides reflecting less than 11% of the light reflected by a polytetrafluoroethylene diffuse reflectance standard in any direction. A view-angle independent black structural colour in snakes is reported here for the first time.**

Colour plays an important role in animal signalling. Intense colours are a tool in mate choice[1–5] and communication[6]. Conspicuous aposematic colouration warns predators of inedibility, i.e. poisonous or venomous prey and is imitated in mimicry[7]. Moreover, colouration enables body temperature control[8–11]. Thus, pigments are widely spread in the animal kingdom. Besides the omnipresent dark melanin also yellowish and reddish pigments are known in many vertebrates, such as reptiles and birds[12–16].

The limited range of these pigmental colours is extended with optical effects based on the surface or/and material structure (structural colours)[17]. In skin and feathers of birds the wide range of colouration can be ascribed to coherent scattering by integumental arrays like spongy keratin matrix[18–20]. In poikilothermic vertebrates iridophores yield hues of white, blue and khaki by the absorption, reflection, refraction and scattering of light[14,15,21]. Iridescence, the phenomenon of viewing angle depending colour shifting, is another structural effect based on coherent scattering. This effect has been convergently evolved in insects, snakes and the feathers of birds[22–33]. While colouration in these examples provides conspicuity, colouration is also applied to prevent detection (crypsis) which is a benefit for animals of prey as well as for predators (aggressive mimicry)[7].

Countershading cancels out shadows originating from directional light (self-shadow concealment) or obliterates the spatial body form of an animal (obliterative shading). Colour, lightness and colouration pattern can be either adapted to the surrounding (background matching) or arranged to markings that blur during motion in order to match the animal's surface in locomotion to the surrounding (flicker-fusion camouflage). Obvious markings, such as geometrical spots, are used to create false edges or boundaries to veil the animal's true outline and shape (disruptive colouration) or to distract the attention of the spectator to parts of the body (distractive markings)[34].

The West African Gaboon viper, *Bitis rhinoceros* (SCHLEGEL, 1855), is by far the largest of the African vipers[35] and the unique colouration makes this species a master of camouflage among snakes. The West African Gaboon viper's skin is divided in sharp contoured hourglass-shaped spots in shades of white, brown and black (Fig. 1a). Intense colouration of black spots is reminiscent of black velvet and purports spatial depth. This results in high-contrast to the pale-coloured rest. Thus, the body contour of the large snake is nearly invisible at the richly-patterned ground of the forest (Fig. 1b).

Snake scales feature specific structures at their surface, so called microornamentation[36]. Skin microornamentation has a great variability in the micro- and nanometre range in different snake species[36–49]. Its taxonomic relevance[40,50] and correlations between microornamentation type, phylogeny and animal's habitat[51] have been


**Figure 1 | *Bitis rhinoceros*, West African Gaboon viper (a) The snake partly on white background and (b) partly on leafy substrate similar to the natural habitat.**

previously discussed. Frictional modulation by ventral microornamentation has been previously shown[52–55]. The role of microornamentation for generating specific optical properties has been assumed since its discovery[38] and is documented for the indigo snake (*Drymarchon couperi*) and fossorial uropeltid snakes. In the first species, the denticulate scale topography acts as diffraction grating generating an iridescent effect[24]. At dorsal scales of representatives of uropeltidae striations with intermediate pits yield diffractive colour ranging from blue to orange[25]. However, microornamentation that enhances pigment based colouration has not been found in snakes so far.

In this study we examined morphology and optical properties of the dorsal skin in the West African Gaboon viper, *B. rhinoceros* in order to reveal possible effects of scale microornamentation on its black appearance. By the use of scanning electron microscopy (SEM), we compared the surface topography of velvet black and pale scales. Optical measurements were carried out to determine their reflectance, transmittance and absorbance characteristics.

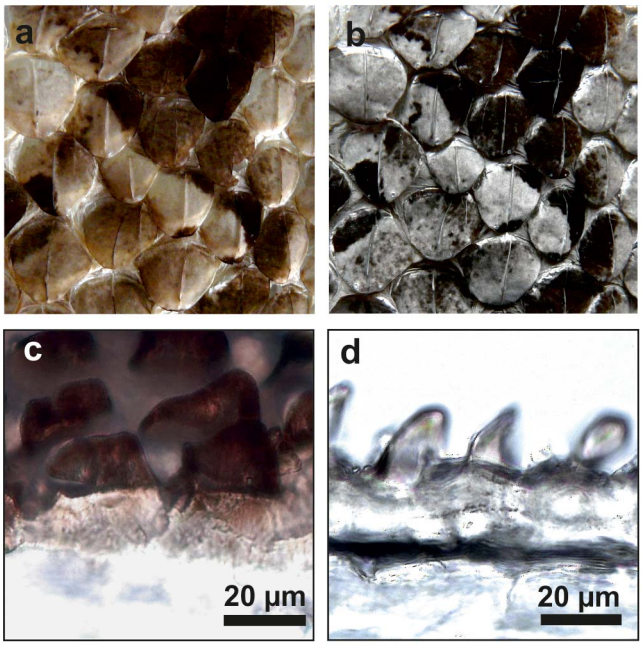


**Figure 2 | Colouration of scales of *B. rhinoceros*.** (a) Dorsal surface of exuvia of *B. rhinoceros*. (b) Same site sputter-coated with a 15 nm thick layer gold-palladium. (c) Light microscopy image of a cross-section from the black part of a dorsal scale of *B. rhinoceros*. (d) Light microscopy image of a cross-section from the pale part of a dorsal scale of *B. rhinoceros*.

## Results

**Morphology.** The original colouration of the West African Gaboon viper partly remains in the shed skin (exuvia). Its dorsal surface has alternating velvet black, light brown, and pale colours (Fig. 2a). The light brown colour is composed of black and whitish dots. In cases where colouration boundaries are not coincide with the scale edges, the colouration changes within one single scale and scales demonstrate sharp colouration boundaries. Ventral scales are yellowish and nearly transparent. After sputter-coating with a 15 nm thick layer of gold-palladium, the dorsal colouration pattern and colour boundaries remained at the exuvia (Fig. 2b). Coated black areas and black dots of the light brown areas appeared black further on. Coated pale areas and dots and ventral scales had a light metallic lustre.

Pale and black areas of exuviae also differed in pigmentation. Under the light microscope dark pigments were solely found in black areas and were only located in the external layers of the integument (Fig. 2c). In pale areas all layers were transparent (Fig. 2d).

SEM images from exuviae of *B. rhinoceros* showed that structuring of scale surfaces coincided with the colouration. Black areas featured a hierarchical micro- and nanostructured surface (Figs. 3a–d). They were covered with leaf-like microstructures (Fig. 3a) consisting of several crests (Fig. 3b). Measured at the tip, the leaf-like structures had an average height of 30 ± 4 µm (mean ± s.d.) and an average density of 1900 ± 100 $mm^{-2}$. These structures were covered by branched ridges at the nanometre scale (Fig. 3c). The ridges averaged

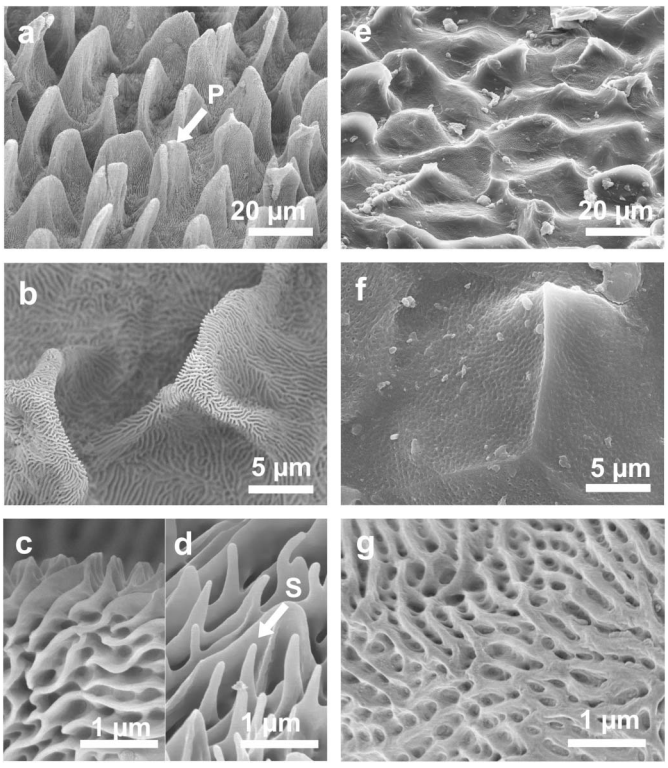


**Figure 3 | SEM images of dorsal scales of *B. rhinoceros*.** (a) Microornamentation at a black dorsal scale, leaf-like structures at the surface (P). (b–c) Branched ridges at the surface of the leaf-like structures at a black dorsal scale. Ridges are regularly connected by thin struts. Pits are located between struts and ridges. (d) Ridges with spinules (S) between the leaf-like structures at a black dorsal scale. (e) Verrucate pattern at a pale dorsal scale. (f–g) Pits on the surface of a pale dorsal scale.

a height of 600 ± 10 nm, thickness of 60 ± 10 nm and were after branching parallel with a distance of 330 ± 50 nm to each other. Their orientation was perpendicular to the contour lines of the leaf-like structures towards the apex and crests (Fig. 3b). Ridges were regularly connected with struts (Fig. 3c). Areas between the leaf-like structures were also covered with the ridges (Fig. 3d). However, in this region ridges featured additionally hair-like protuberances (spinules, Fig. 3d). Pale scale sites featured a verrucate surface with lower elevations of 10 ± 1 μm average height (Fig. 3e). The average density of these elevations (2000 ± 200 $mm^{-2}$) was similar to that found in leaf-like structures (t-test, P = 0.219). Elevation surfaces were interspersed with nanoscaled pits (Fig. 3f, g).

**Optical characteristics.** The reflectance spectra of ventral scales, dorsal pale sites, dorsal black sites and of 15 nm thick Au-Pd coated scales are shown in Fig. 4. The reflectance of pale scales and black dorsal scales was different in the spectral range 250–950 nm. Depending on the wavelength, pale scales reflected 16–70% (median: 26.7%) of the diffuse polytetrafluoroethylene reflectance standard. In contrast, black scales reflected only 4.0– 58.0% (median: 10.8%). Pale scales reflected stronger than black ones in the whole analysed spectral range (Wilcoxon Signed Rank (WSR) Test, P = <0.001). The reflectance of both scale types increased with an increasing wavelength and reached its maximum at the wavelength of 880 nm. Differences in reflectance between pale and black scales were higher at short wavelengths below 600 nm (Fig. 4b). This is apparent in the different slope of reflectance spectra for increasing wavelengths (Fig. 4a). For instance, black scales reflected less than 25% at wavelengths ranging from 500 to 600 nm compared to pale scales (Fig. 4b).

Also metal coated black and pale sites on scales maintained similar reflection characteristics (Fig. 4a). However, coated pale scales (median: 55.5%) were stronger reflectors than uncoated pale scales (WSR Test, P = <0.001) and the reflectance of coated pale scales was as high as that of uncoated ventral scales (median: 55.2%). On the contrary, metal coating of black scales effected the decrease of their reflectance (median: 3.5%). In contrast to uncoated black scales, a low reflectance (mean: 3.4%) was observed in coated black scales for a wide spectral range 300–800 nm.

In Fig. 5 we present the scattering properties of black and pale snake scales and scattering properties of a rough surface in accordance to the Oren – Nayar model[56] (Fig. 5c). The angular dependence of light scattering of black and pale scales at 45° illumination (Fig. 5a) was different (Fig. 5b–f). As in the previous measurement, intensity of scattered light of the pale scales was higher than in the black scales (Fig. 5b, e). Such a difference was observed in both cases, when sensor and irradiation source were oriented laterally and rostro-caudally to the scales (Fig. 5d–f).

In addition to their differences in total scattering and reflection, black and pale scales featured also contrary properties of angle dependent scattering. The pale scales featured a main direction of reflected light (700 nm) at angles 40–60° (Fig. 5c, d). The intensity of the scattering light, measured at these detection angles, was higher than the intensity detected from other angles in the whole spectral range. The lowest scattering intensity was measured at angles of 0° and 80° (Fig. 5c, d). In black scales the highest intensity of scattered light was measured at low angles of detection (<40°), corresponding with a higher rate of scattering perpendicular to the surface (Fig. 5e, f). At higher angles to the surface's normal, corresponding with a horizontal view on the scales, the detected intensity decreased continuously (Fig. 5e, f). Although angle-dependent distribution of intensity was similar in both laterally and rostro-caudally orientation of scales to the sensor and source of irradiation, in both black and pale surfaces the variation of intensity over the detection angles was higher in rostro-caudal arrangement (Fig. 5d, f). In these cases, the range between the maxima and minima of the intensity curves was larger (Fig. 5d, f).

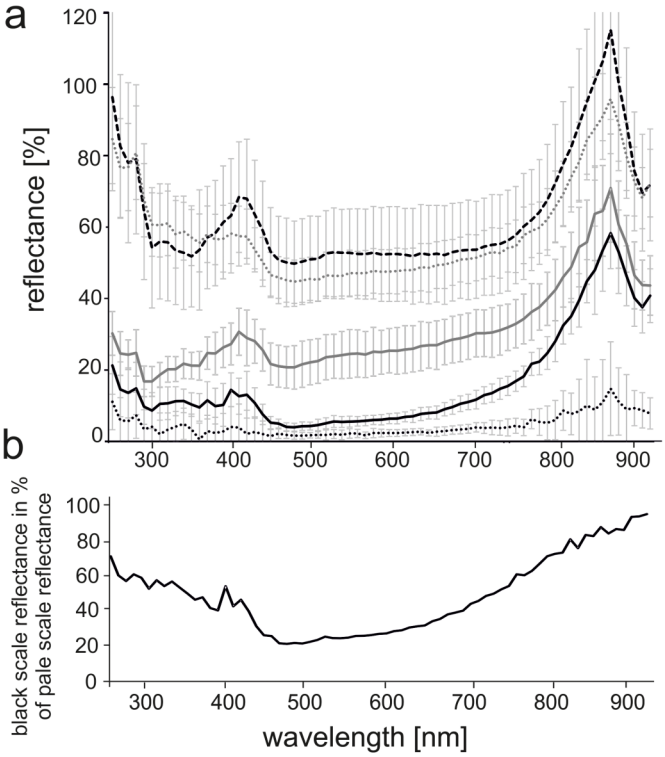


**Figure 4 | Reflectance of the scales of *B. rhinoceros*.** (a) Reflectance of black dorsal scales (black line), Au-Pd coated black dorsal scales (dotted black line), pale dorsal scales (grey line), Au-Pd coated pale dorsal scales (dotted grey line), and ventral scales (dashed black line) of *B. rhinoceros* in percent to the reflected light of the diffuse reflectance standard. Standard deviation of all ten scales measured is presented by error bars. (b) Reflectance of black dorsal scales in percent to the reflectance of pale scales.

The run of our fitted curve differed from scattering curves of both biological surfaces (Fig. 5c). In the model, we obtained the best fit in the case when the angles of the v–shape cavities[56] of the model surface were not normally distributed (Gaussian distribution), but homogenously (homogenous distribution). A maximum of intensity as observed in pale scales indicating specular reflection was not predicted by the model. In the model, the intensity of scattered light increases with increasing angle (Fig. 5c). Such angle-dependent scattering is contrary to the black scales of the snake (Fig. 5f).

Different scale types showed also different transmittance (the ratio of the transmitted to incident irradiance). Data for the uncoated ventral scales, uncoated and Au-Pd coated dorsal black and pale scales are presented in Fig. 6. The nearly transparent ventral scales transmitted more than 58% of light in the measured spectral range (Fig. 6a). Uncoated pale scales transmitted 8–28% of the incident light (Fig. 6a). After Au-Pd coating, transmittance of pale scales decreased by one half (Fig. 6a). In comparison to uncoated pale scales, coated and uncoated black scales transmitted less radiation, particularly in the wavelength range of 400–900 nm (Fig. 6b). Black and pale scales of *B. rhinoceros* had also different absorption characteristics. After one minute long warming up by electrical lamp illumination (near UV - visible light), dark areas of the exuvia were on average 2°C warmer than pale areas (Fig. 7).

## Discussion

The microornamentation in velvet black regions of the Gaboon viper skin is unique among snakes. Leaf-like microstructures with both nanoridges and hair-like nanoprotuberances that coincide with black skin colouration have never been described before. Close relatives of the West African Gaboon viper, the western many-horned adder,

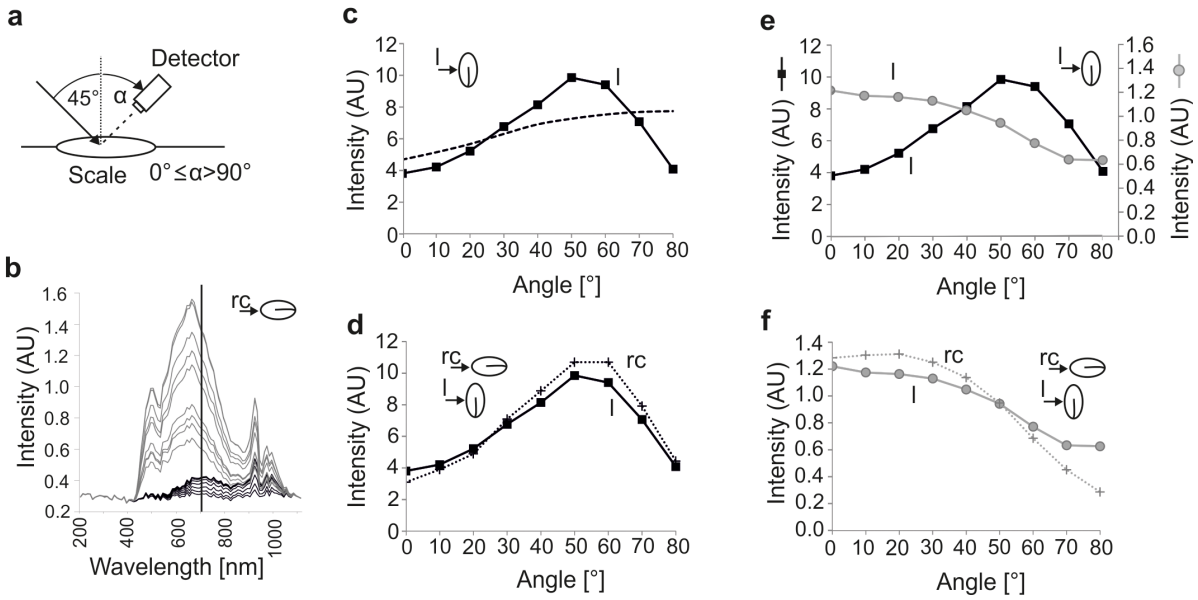


**Figure 5 | Scattering measured on scales of *B. rhinoceros* and predicted by the Oren – Nayar model[56].** (a) Schematic drawing of the experimental setup for the measurement of light scattering. Intensity of scattered light was measured at different angles in respect to the scale surface normal: 0°–80° with an illumination angle at 45°. (b) Raw reflection spectra of a black (black lines) and a pale (grey lines) scale with illumination and detector arranged in the rostro-caudal direction (rc) detected from different angles. The intensity of scattered light is presented in arbitrary units. (c) Comparison between light scattering for a pale scale at 700 nm detected from lateral direction (solid line) and light scattering predicted by the model (dashed line). As fit parameters $\rho E_0 = 37$ and $\sigma = 17.5$ were applied. The light scattering intensity has the same units as in (b). (d) Intensity of light scattering for a pale scale at 700 nm detected from caudal (rc, dotted line) and lateral (l, solid line) direction. The intensity has the same units as in (b). (e) Comparison of the light scattering intensity of a pale (y-axis on the left, black line) and a black (y-axis on the right, grey line) scale at 700 nm detected from lateral direction. The intensity has the same units as in (b). (f) Light scattering angular dependence of a black scale detected from caudal (rc, dotted line) and lateral (l, solid line) direction at 700 nm. The intensity has the same units as in (b).

*Bitis caudalis*[51], and the mountain adder, *B. atropos*[57], feature only a less complex dorsal pattern of lower microscaled elevation with pits. This structuring is similar to that of the pale regions of *B. rhinoceros*. Location of the leaf-like microstructures in the West African Gaboon viper and their dimensions in the range of visible light wavelengths suggest the contribution of microornamentation to the velvet black appearance. Gold-palladium coating on relatively flat ventral scales turns it to the metallic appearance. In contrast to this, after coating of dorsal black and pale scales, the colouration contrast remains because coated black sites remain black. Consequently, the surface structures of the black scales must be responsible for the velvet black appearance or at least enhance it.

According to the conservation law, incident light is reflected, transmitted, or absorbed by a sample. Absorbance ability is important for surface′s dark appearance. The theoretical darkest surface, an ideal black body, is a total absorber, which absorbs incident light and does not reflect or transmit any radiation[58]. Since pale scales reflect and transmit more light than black scales, especially the wavelength range 400–700 nm, black scales must absorb more light than pale scales. According to Kirchhoff′s law of thermal radiation, at thermal equilibrium, the emissivity of a body or surface equals its absorptivity[58]. In the West African Gaboon viper, the resulting emitted heat of the absorbing black areas was detectable by IR imaging. As there is no solid evidence in the literature that the arrangement and material of adjacent scales are different in snakes, the faster heat up process of black scales in comparison to pale scales must be solely caused by their pigmentation and surface structure.

The hierarchical microornamentation of the West African Gaboon viper′s black scales gains the pigmental absorbance. Incident light is reflected multiply and scattered by surface irregularities in the nano- and micrometre range (light trapping). In any case, one part of the incident (or previously by the structures scattered or reflected) light could be absorbed by dark pigments that are deposited within the uppermost layers of skin[59]. However, our data show that absorbing pigments are not the main reason for the black appearance of the snake scales. The refractive index of a material and its relation to that of the surrounding medium is the decisive factor which defines whether electromagnetic radiation is reflected or led into the material where it can be absorbed. The refractive index of the snake′s epidermal material mainly consisting of α- and β-keratin[60] can be estimated as that of the keratin of birds (refractive index 1.56)[61,62], which is lower than that of metal. As known from the structures on the wings of butterflies[63], the intrinsic refractive index of the epidermis of black scales of *B. rhinoceros* can be shifted by the nanostructures in wavelength dimension. Thereby surface structuring influences the rate of reflection and transmission which corresponds to the absorption. In our measurements, metal coated black snake scales maintained their black colouration and became even less reflective than the untreated scales. Considering the high refractive index of metal, the ultrablack appearance might not be due to the effect of pigment absorption. The dark colouration must be rather caused by a structure-based increase of the refractivity.

In order to confirm the nanostructures′ responsibility for the appearance of black snake scales, we compared the angle dependence of scattering of snake scales with calculated data from an established model for reflection of a surface with microscopic v-shaped cavities[56]. The model parameters were selected to obtain the best fit to the biological surface. Whereas the model provided an approximation for the scattering properties of pale scales, particularly with homogenous distribution of cavity angles, for the black surfaces it failed and even led to contrary results with regard to the scattering at small and large angles. These differences can be only explained by the effect of nanostructures, which is not considered in the model of Oren and Nayar[56].

In both black and pale scales angle-dependent scattering was nearly similar in both orientations. This can be explained with the

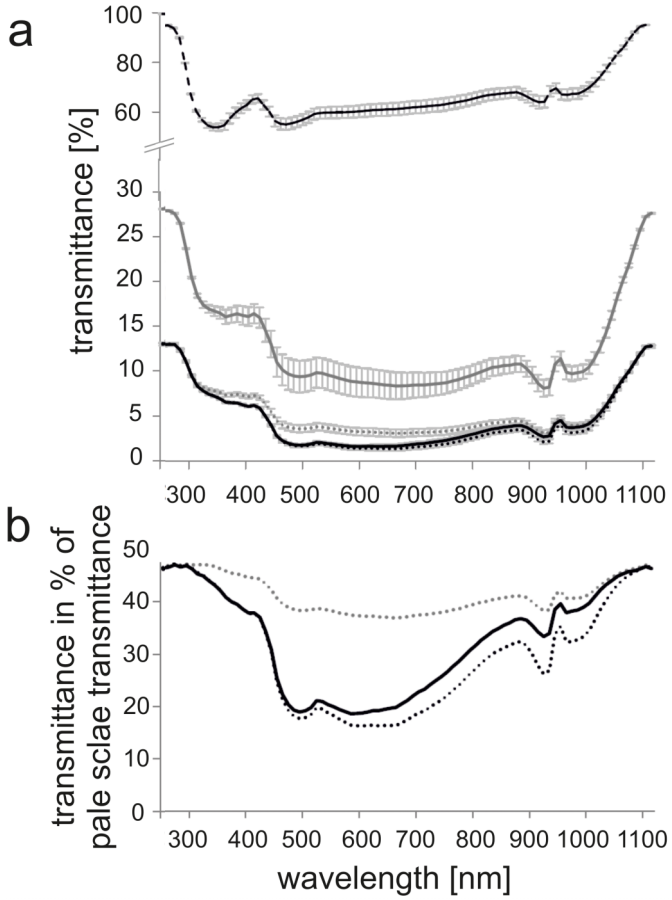


**Figure 6 | Transmittance of scales of *B. rhinoceros*.** (a) Transmittance spectra of black dorsal scales (black line), Au-Pd coated black dorsal scales (dotted black line), pale dorsal scales (grey line), Au-Pd coated pale scales dorsal (dotted grey line), and ventral scales (dashed black line) of *B. rhinoceros*. Standard deviation of ten scales measured is presented by error bars. (b) Transmittance of black dorsal scales (black line), Au-Pd coated black dorsal scales (dotted black line) and Au-Pd coated pale dorsal scales (dotted grey line) in percent to the pale scale transmittance.

nearly isotropic arrangement of leaf-like structures, crests and nanoridges. Slightly differences can be explained by a low degree of orientation of micro- and nanostructures toward the axis of the snake's body.

The term "velvet-like" is used in many contexts, in scientific publications as well as in the everyday language. Velvet tissue fascinates in many respects. Its intrinsic gloss (velvet gloss) only occurs at certain angles[64]. At all other angles the low reflecting velvet shows high colour saturation and appears darker than other materials (velvet effect). Similar characteristics also occur in plants. At petals of *Viola tricolor hortensis* (pansy) and *Primula sinensis* papillate structures that are filled with a pigment containing cellular fluid and covered by a pellucid reflecting cuticle lead to a deep colour that change into a velvet-like gloss depending on illumination and viewing angle[65,66]. The West African Gaboon viper′s black scales feature a low-reflecting black colouration for a large range of incident wavelengths. Regarding this, black scales have a velvet effect. However, low reflectance is maintained for any viewing angle. According to this, the optical properties of Gaboon viper′s black scales differ from that of glossy velvet. In animal kingdom a hierarchically structured surface, like the microornamentation at black scales of the Gaboon viper causing low-reflectance, is unique and only comparable with the structures responsible for ultra-black in butterflies. *Papilio ulysses* features a hierarchical structured surface which enhances pigmental blackness[63]. A microscopic lattice of struts and walls between a periodic ridging of pitch about 2–3 μm and densely distributed lattice of cuticle underneath these structures scatter incident light towards the diffuse distributed pigmentation. Additionally, nanoscopic ridges on the ridging in subwavelength range are hypothesized to function as impedance matching elements[63]. In contrast to the butterfly, the West African Gaboon viper's microornamentation is isotropic at micro- and nanoscale and not arranged in several layers. This feature causes suppression of specular reflection. However, the physical principle of the guiding of incident light towards embedded absorbing pigments is fundamental for both the snake′s and butterfly′s system. This effects the low-reflectance of these surfaces.

The benefits of structures enhancing black colouration in snakes seem to be obvious. However, biological surfaces are generally multifunctional. Ecology and lifestyle of species may suggest the functions of their morphologic features but are always speculative.

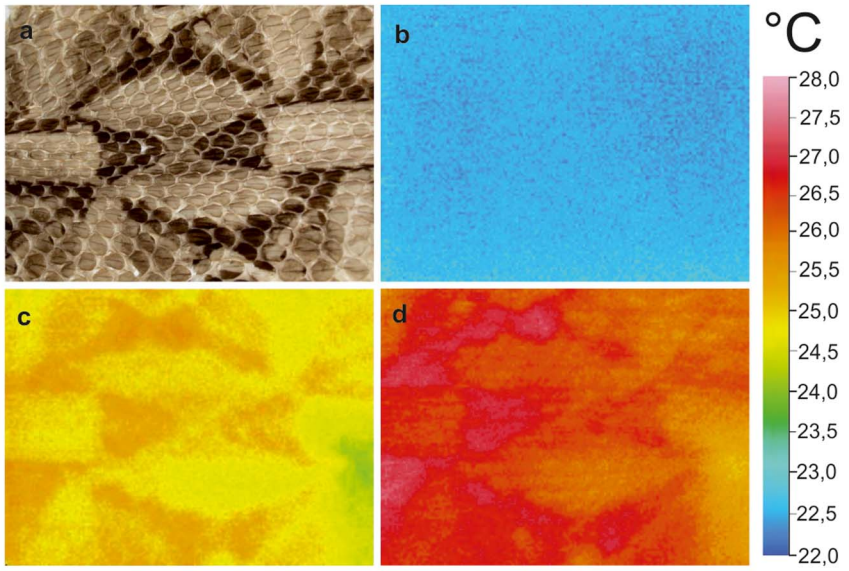


**Figure 7 | Warm-up process of the exuvia of *B. rhinoceros*.** (a) Exuvia of *B. rhinoceros*, West African Gaboon viper. (b) IR-emission image of the exuvia of *B. rhinoceros* before illumination under ambient room conditions temperature, (c) after 1 min illumination, and (d) after 2 min illumination.

The West African Gaboon viper inhabits West Africa from Togo to Guinea[67]. It lives at margins of and within the tropical rainforest, in swamp areas and near water streams[35,67]. But also anthropogenic habitats like plantations and secondary forest are inhabited. *B. rhinoceros* is recognized as separate species only recently[68–70] and has previously been a subspecies of *Bitis gabonica*. As its relative *B. gabonica*[71], *B. rhinoceros* is a terrestrial nocturnal ambusher sitting for hours in the vegetation and waiting for birds and mammals, especially in nightfall[30]. Prey is captured with one final fast strike and killed by the injection of venom by the fangs[72]. If the snake feels threatened, it hisses loudly by the expiration of each breath[35,72]. The camouflage of the snake on the rainforest floor plays a key role for hunting as well as for the prevention of becoming food to other animals.

Taking into account the West African Gaboon viper's biology, velvet black colouration suggests to be a tool for a perfect camouflage. The disruptive geometrical colouration pattern of pigment based colours conceals the body contours and makes the snake on the ground of the forest indistinguishable. Such colouration was interpreted as common concealing pattern in large stationary snakes[73]. In addition, the West African Gaboon viper is camouflaged by areas with alternating reflectance due to different microornamentation at the scale surfaces, the obliterative shading. This pattern of alternating reflectance coincides with that of colouration. Thus, the viper features black spots with low reflectance, that purport spatial depth and pale areas that reflects the incident light. This high-contrasting pattern is a perfect camouflage in the richly-structured forest ground with variations of light and shade originated by the canopy. Beside optical characteristics of skin and visual system of the observer, colour appearance of an animal also depends on the spectrum of ambient light[7,74,75]. In the West African Gaboon viper reflectance contrast of pale and black spots is higher for short wavelengths (corresponding with bluish and greenish colour) than for longer ones. Data about ambient illumination have been collected in numerous studies. Under the open sky, regardless whether cloudy or clear, radiance spectra are dominated for wavelengths longer than 500 nm[76,77]. Under these conditions differences in reflectance between black and pale spots would be rather low. However, considering the snake′s habitat, spectral reflectance characteristics of its skin are quite beneficial: Radiance spectra of forests at many continents show a radiance intensity peak at 550 nm (green), due to direct transmission and reflection of the canopy[77,78]. Under clear sky, woodlands and forests with larger gaps in their canopies shift the spectra of ambient light towards shorter wavelength (blue)[77]. Low sun angles at dusk and dawn in combination with the absence of clouds lead to deficiency of the wavelength range from 630 to 750 nm and consequently overrepresentation of bluish light and long wavelengths corresponding to the red colour. Although these spectral data[77] do not include the viper′s African habitat, based on similarity of data in previously forest studies, the results can be presumed for the African rainforest. All mentioned spectra share a high contribution of short wavelengths. Especially this range is reflected differently by pale and black areas. This yields a high-contrast in reflectance, which camouflages the snake especially during ambushing in the evenings. But the system also provides high-contrasting appearance at day time in the greenish light of the forest or the bluish light of woodland and open anthropogenic vegetation.

In our measurements dorsal pale and black scales were transparent in the measured UV range, especially for shorter wavelengths. Because radiation of this spectral range was less reflected by these scales, it can be assumed that UV radiation is at least able to pass through the shed upper skin layers. For a species that lives at the bottom of forests and woodlands, where the main part of the destructive UV radiation is reduced; such properties may ensure sufficient UV supply for vitamin D3 synthesis. Our findings do not correspond with data on transmissivity[78] and reflectance[79,80] of the epidermis in other reptiles showing that reptile skin strongly absorbs the ultra violet and transmit the visible range of the solar spectrum. Comparisons with transmittance spectra of colubrid, boid and pythonid snakes show that even the epidermis of arboreal species is not nearly as transparent for ultra-violet and blocks less visible and infra-red radiation as the epidermis of the West African Gaboon viper[78].

However, different characteristics of reflectance in dorsal and ventral skin of different lizard and snake species suggested that, beside solar protection, also thermoregulation and concealment are selective factors for epidermal reflectance in reptiles[79,80].

The West African Gaboon viper′s low reflecting properties were preserved even when scale structuring was covered with gold-palladium. Thus, the structure based velvet black effect could also be potentially transferred to other materials. In science and technology such high-absorbing and low-reflecting surfaces are of prime importance and can be applied in many fields, such as solar thermal collectors or optical systems. Increasing interest in such materials is reflected in a growing number of recent publications about ultra-black surfaces that avoid any reflectance and absorb nearly any incident light[81]. The currently darkest commercially established surface is a nickel phosphorous alloy[82]. The low-reflecting properties of this material can be enhanced by modifications of the surface topography. Different phosphorous contents cause different surface structures appearing in the acid etching process. The reflectance can be less than 0.4%[82]. The currently darkest surface is made of vertically aligned carbon nanotubes (VACNT) which reflect 0.045% of incident light[83]. A large amount of recent publications studied the optical properties and optimization of fabrication of these materials[84–86]. The structures are fragile. But research continually creates new ultra-dark high absorbing materials such as silicon nanowires arrays (SiNWAs)[87], laser textured metals[88], nanoporous anodised aluminium oxide-coated polycarbonate surfaces[89] and graphene sheet stacks[90]. Overall, these studies demonstrate the strong influence of surface topography on material′s reflectance and absorption. The surface topography of the West African Gaboon viper's velvet black scales resemble the ultralow reflectance ultrafast laser textured metal surfaces of Iyengar and his co-workers[88]. Both surfaces feature leaf-like structures or pillars[88] in a similar range with an average diameter of about 20 μm and an average height of about 30 μm. Both materials feature nearly angle independent reflection characteristics. Further, in both cases the coverage with an absorbing layer decreases the reflectance.

Nonetheless, the West African Gaboon viper′s microornamentation might enhance the darkness of artificial materials. Especially varying orientation of the nanoridges could be an inspiration for engineering ultra-black designer. The microornamentation on the snake′s velvet black scales is a further example that the same physical law applies to both nature and technology and leads consequently to similar constructions. Regarding to the relation of durability and weight the fine shaped structures of the West African Gaboon viper are not inferior to artificial ultra-black surfaces considering that the snake slithers several month until the next shedding with its fine structured skin on the undergrowth.

## Methods

**Microscopy.** Surface topography was examined in exuviae from two individuals of *Bitis rhinoceros* obtained from Tierpark Hagenbeck gGmbH, Hamburg, Germany, and from a private keeper. Microornamentation was determined from SEM images of the exuviae. Single scales and hand made cross-sections of scales were mounted on aluminum stubs by using double-sided carbon conductive tape (Plano, Wetzlar, Germany) and sputter coated in a BAL-TEC SCD 500 Sputter Coater using a BAL-TEC QSG 100 Quartz Film Thickness Monitor (Bal-tec AG, Balzers, Lichtenstein) with 15 nm thick gold-palladium. After preparation samples were studied in a scanning electron microscope Hitachi S-4800 (Hitachi High-Technologies Corp., Tokyo, Japan) at an accelerating voltage of 3 kV. Quantitative surface data were obtained from images with the free image processing program image J 1.44. Density of elevations at pale scale areas and leaf-like structures at black areas were measured from top view images. The height of elevations and leaf-like structures was determined from the cross-sections. Dimensions of ridges were measured from cross-sections and top view images. The density of the structures was determined of three

scales per individual. For the height of the microstructures and the dimensions of the nanoridges, five values were taken from one scale. Five scales per individual were examined. Light microscopy images were taken with a Zeiss Axioplan (Carl Zeiss MicroImaging GmbH, Jena, Germany) with a camera (Zeiss AxioCam MRc, software Zeiss AxioVision 3.1, Carl Zeiss MicroImaging GmbH, Jena, Germany). Therefore manual sliced cross-sections of dorsal black scales and pale scales were mounted in water on a glass slide and covered by a cover slip.

**Infra-red imaging.** For infrared imaging an exuvia of one individual was placed on a 2 cm thick polystyrene plate (heat insulator) at room temperature. IR images were taken with an IR camera (IR FlexCam® T with GTS Thermography Studio 4.7, GORATEC Technology GmbH, Erding, Germany) before, during and after a heat up process generated by a 10 min enduring irradiation with a 100 W light bulb (UV Reptile vital, Hobby, Dohse Aquaristik KG, Gelsdorf, Germany) at 20 cm distance.

**Measurement of reflectance, scattering and transmittance.** Optical characteristics of the snake epidermis were measured at the exuviae of one individual used for the SEM study. In 90° reflectance measurement a balanced deuterium tungsten halogen light source (DH-2000-BAL, Ocean Optics Inc, Dunedin, Florida, USA) produced light from ultraviolet to near infrared (wavelength range from 200 to 1100 nm). Light was guided to the surface through an optical fibre with the diameter of 200 µm. The fibre output was placed 2 mm above the scale surface. The reflected light was collected and directed to the monochromator (Ocean Optics Inc, Dunedin, Florida, USA) by an optical fibre. Data were recorded with the software Spectral Suite (Ocean Optics Inc, Dunedin, Florida, USA). With this arrangement the 90° reflectance spectra of ten dark dorsal, ten pale dorsal and ten ventral scales was determined.

The same measurements were done with scales sputter-coated with 15 nm thick layer gold-palladium. Sputter coating was done with the sputter coater described above. Placement of the scales above a dark chamber during experiment prevented detection of backscattered light which might potentially pass though the partially pellucid scales. The measured reflectance of the snake scales were presented in percents of the reflectance of the diffuse reflectance standard (reference white, WS-1-SS, Mikropack GmbH, Ostfildern, Germany), which was also measured ten times and then used for each incidence wavelength as reference value corresponding to 100% reflectance.

Transmission measurements were performed with the same setup. The scale was placed between the light source and the sensor. For this purpose, a glass fibre with a collecting lens was placed directly underneath the scale and connected to the collimator attached. The output fibre was placed 9 cm above the scale surface and supplied with an achromatic collimator lens. With this setup, transmission spectra of ten scales of each type, Au-Pd coated and uncoated dorsal black, dorsal pale and ventral scales were measured. Transmittance values were calculated as a ratio of the irradiance passing though the sample to the intensity of incident radiation. For the measurement of the angular dependence of reflectance, the output fibre was fixed at an angle of 45° and at a distance of 5 cm from the scale surface. The input fibre with a collimator lens was placed at a test angle at fixed distance of 13.5 cm from the scale on a guiding rail. Intensity of scattered light could be measured from different angles (0°–80°) (Fig. 5a). Reflection measurements were done with black and pale dorsal scales mounted on low-reflecting dark velvet oriented laterally (l) or rostro-caudally (rc) to the light source (Fig. 5c–f). The setup for other measurements was similar to the setup for the transmission measurements, except for spectral measurements for which the halogen light source was used.

**Calculation of angle dependent light scattering.** We compared our measured angle dependent reflectance with calculations for a model surface according to the Oren – Nayar model[65], which is supported by experimental studies and is an established model in computer vision. This model describes diffuse reflection from the surfaces with Lambertian symmetric v-shaped cavities, whose upper edges are in a plain. The width of the cavities is assumed to be small in comparison to their length. Reflection from the both facets of each cavity is considered in the model. Surface roughness is modelled by the Gaussian distribution of facet slopes, which is defined by the mean µ and the standard deviation σ. In this model, the direction of illumination is defined by the angle $\theta_i$ to the surface normal and by the azimuth angle $\Phi_i$ to the x-axis in the surface plain. A detection direction is defined by the angle $\theta_r$ to the surface normal and by the azimuth angle $\Phi_r$ to the x-axis in the surface plain. According to Oren and Nayar[65] the surface radiance is defined as follows:

$$L_r^1(\theta_r,\theta_i,\Phi_r-\Phi_r;\sigma)=\frac{\rho}{\pi}E_0\cos\theta_i[C_1(\sigma)+\cos(\Phi_r-\Phi_i)C_2(\alpha;\beta;\Phi_r-\Phi_i;\sigma)\tan\beta+(1-|\cos(\Phi_r-\Phi_i)|)C_3(\alpha;\beta;\sigma)\tan\left(\frac{\alpha+\beta}{2}\right)] \quad (1)$$

with the following coefficients:

$$C_1=1-0.5\frac{\sigma^2}{\sigma^2+0.33} \quad (2)$$

$$C_2=f(x)=0.45\frac{\sigma^2}{\sigma^2+0.09}\sin\alpha \quad (3)$$

$$C_3=0.125\left(\frac{\sigma^2}{\sigma^2+0.09}\right)\left(\frac{4\alpha\beta}{\pi^2}\right)^2 \quad (4)$$

where $\alpha = \max[\theta_r, \theta_i]$ and $\beta = \min[\theta_r, \theta_i]$, $E_0$ is the irradiance when the facet is illuminated head-on, $\rho$ is the fraction of incident energy reflected by the surface (albedo).

The interreflection between neighbours facets may be taken into account according:

$$L_r^2(\theta_r,\theta_i,\Phi_r-\Phi_r;\sigma)=0.17\frac{\rho^2}{\pi}E_0\cos\theta_i\frac{\sigma^2}{\sigma^2+0.13}\left[1-\cos(\Phi_r-\Phi_i)\left(\frac{2\beta}{\pi}\right)^2\right] \quad (5)$$

For the fit of our experimental angle dependent light scattering the interreflection was considered.


1. Hill, G. E. Female house finches prefer colourful males: sexual selection for a condition-dependent trait. *Anim. Behav.* **40**, 563–572 (1990).
2. Hill, G. E. Female mate choice for ornamental coloration. In *Bird Coloration: Vol. 2, Function and evolution* (Harvard University Press, Chambridge, 2006).
3. Milinski, M. & Bakker, T. C. M. Female sticklebacks use male coloration in mate choice and hence avoid parasitized males. *Nature* **344**, 330–333 (1990).
4. Watkins, G. G. Inter-sexual signalling and the functions of female coloration in the tropidurid lizard *Microlophus occipitalis*. *Anim. Behav.* **53**, 843–852 (1997).
5. Parker, A. R., Mckenzie, D. R. & Ahyong, S. T. A unique form of light reflector and the evolution of signalling in Ovilipes (Crustacea: Decapoda: Portunidae). *Proc R Soc Lond B* **265**, 861–867 (1998).
6. Stuart-Fox, D. & Moussalli, A. Selection for social signalling drives the evolution of chameleon colour change. *Plos. Biol.* **6**, 22–28 (2008).
7. Endler, J. A. An overview of relationships between mimicry and crypsis. *Biol J Linn Soc Lond* **16**, 25–31 (1981).
8. Cole, L. C. Experiments on toleration of high temperature in lizards with reference to adaptive coloration. *Ecology* **24**, 94–108 (1943).
9. Pearson, O. P. The effect of substrate and skin color on thermoregulation of a lizard. *Comp. Biochem. Physiol.* **58**, 353–358 (1977).
10. Sherbrooke, W. C. & Frost, S. K. Integumental chromatophores of a color-change, thermoregulating lizard, *Phrynosoma modestum* (Iguanidae; Reptilia). *Am. Mus. Nov.* **2943**, 1–14 (1989).
11. Walton, B. M. & Bennett, A. F. Temperature-dependent color change in Kenyan chameleons. *Physiol. Zool.* **66**, 270–287 (1993).
12. Blair, J. A. & Graham, J. The pigments of snake skins. *Biochem. J.* **56**, 286–287 (1954).
13. Fox, D. L. *Animal Biochromes and Structural Colors* (Berkeley: University of California Press, 1976).
14. Bechtel, H. B. Color and pattern in snakes (Reptilia, Serpentes). *J. Herpetol.* **12**, 521–532 (1978).
15. McGraw, K. J. Mechanics of carotenoid-based coloration. *Bird Coloration: Vol. 1, Mechanisms and measurements* (Harvard University Press, Chambridge, 2008).
16. McGraw, K. J. 2008 Mechanics of melanin-based coloration. *Bird Coloration: Vol. 1, Mechanisms and measurements* (Harvard University Press, Chambridge, 2008).
17. Parker, A. R. 515 million years of structural colour. *J. Opt. A: Pure Appl. Opt.* **2**, R15–R18 (2000).
18. Prum, R. O., Torres, R. H., Willamson, S. & Dyck, J. Coherent light scattering by blue feather barbs. *Nature* **396**, 28–29 (1998).
19. Prum, R. O. & Torres, R. Structural colouration of avian skin: convergent evolution of coherently scattering dermal collagen arrays. *J. Exp. Biol.* **206**, 2409–2429 (2003).
20. D'Alba, L. *et al.* Colour-producing β-keratin nanofibres in blue penguin (*Eudyptula minor*) feathers. *Biol. Lett.* **7**, 543–646 (2011).
21. Bagnara, J. T., Fernandez, P. J. & Fujii, R. On the blue coloration of vertebrates. *Pigm. Cell. Res.* **20**, 14–26 (2007).
22. Rayleigh, L. Studies of iridescent colour, and the structure producing it. IV. Iridescent Beetles. *P. R. Soc. Lond. A – Conta* **103**, 233–239 (1923).
23. Rayleigh, L. The iridescent colours of birds and insects. *P. R. Soc. Lond. A – Conta* **128**, 624–641 (1930).
24. Monroe, E. A. & Monroe, S. E. Origin of iridescent colors on the indigo snake. *Science* **159**, 97–98 (1968).
25. Gans, C. & Baic, D. Regional specialization of reptilian scale surfaces: Relation of texture and biologic role. *Science* **195**, 1348–1350 (1977).
26. Parker, A. R. Discovery of functional iridescence and its coevolution with eyes in the phylogeny of Ostracoda (Crustacea). *Proc. R. Soc. B* **262**, 349–355 (1995).
27. Vukusic, P., Sambles, J. R., Lawrence, R. C. & Wootton, R. J. Now you see it - now you don't. *Nature* **410**, 36 (2001).
28. Lawrence, C., Vukusic, P. & Sambles, R. Grazing-incidence iridescence from a butterfly wing. *Appl. Opt.* **41**, 437–441 (2002).
29. Prum, R. O., Quinn, T. & Torres, R. Anatomically diverse butterfly scales all produce structural colours by coherent scattering. *J. Exp. Biol.* **209**, 748–765 (2006).
30. Ingram, A. L. & Parker, A. R. A review of the diversity and evolution of photonic structures in butterflies, incorporating the wok of John Huxley (The Natural History Museum, London from 1961 to 1990). *Phil. Trans. R. Soc. B* **363**, 2465–2480 (2008).
31. Ingram, A. L., Lousse, V., Parker, A. R. & Vigneron, J. P. Dual gratings interspersed on a single butterfly scale. *J. R. Soc. Interface* **5**, 1387–1390 (2008).
32. Doucet, S. M. & Meadows, M. G. Iridescence: a functional perspective. *J. R. Soc. Interface* **6**, 115–132 (2009).
33. Meadows, M. G. *et al.* Iridescence: views from many angles. *J. R. Soc. Interface* **6**, 107–113 (2009).

34. Stevens, M. & Merilaita, S. Animal camouflage: current issues and new perspectives. *Phil. Trans. R. Soc. B* **346**, 423–427 (2009).
35. Spawls, S. & Branch, W. R. *The dangerous snakes of Africa* (Blandford Press Ltd, London, 1995).
36. Picado, C. Epidermal microornaments of the crotalinae. *Bull. Antivenin Inst. Am.* **4**, 104–105 (1931).
37. Leydig, F. Ueber Organe eines sechsten Sinnes. Zugleich als Beitrag zur Kenntnis des feineren Baus der Haut bei Amphibien und Reptilien. *Nova Acta Academiae Caesareae Leopoldino-Carolinae Germanicae Naturae Curiosorum* **34**, 108–110 (1868).
38. Leydig, F. Über die äusseren Bedeckungen der Reptilien und Amphibien. *Archiv für mikroskopische Anatomie* **9**, 753–794 (1873).
39. Pockrandt, D. Beiträge zur Histologie der Schlangenhaut. *Zool. Jb. Anat.* **62**, 275–322 (1936).
40. Hoge, A. R. & Santos, P. S. Submicroscopic structure of "stratum corneum" of snakes. *Science* **118**, 410–411 (1953).
41. Bea, A. Contribución a la sistemática de vipera seoanei lataste, 1879 (reptilia, viperidae) 1. Ultraestructura de la cutícula de las escamas. *Butlletí de la Institució Catalana d'Història Natural* **42**, 107–118 (1978).
42. Lillywhite, H. B. & Maderson, P. F. Skin structure and permeability. In *Biology of the Reptilia* (Academic Press, London, 1982).
43. Price, R. Microdermatoglyphics - the Liodytes-Regina problem. *J. Herpetol.* **17**, 292–294 (1983).
44. Stille, B. Dorsal scale microdermatoglyphics and rattlesnake (*Crotalus* and *Sistrurus*) phylogeny (Reptilia: Viperidae: Crotalinae). *Herpetologica* **43**, 98–104 (1987).
45. Chiasson, R. B. & Lowe, C. H. Ultrastructural scale patterns in *Nerodia* and *Thamnophis. J. Herpetol.* **23**, 109–118 (1989).
46. Chiasson, R. B., Bentley, D. L. & Lowe, C. H. Scale morphology in *Agkistrodon* and closely related crotaline genera. *Herpetologica* **45**, 430–438 (1989).
47. Price, R. & Kelly, P. Microdermatoglyphics - Basal patterns and transition zones. *J. Herpetol.* **23**, 244–261 (1989).
48. Gower, D. J. Scale microornamentation of uropeltid snakes. *J. Morphol.* **258**, 249–268 (2003).
49. Joseph, P., Mathew, J. P. & Thomas, V. C. Scale morphology, arrangement and micro-ornamentation in *Xenochrophis piscator* (Schneider), *Naja naja* (Linn), and *Eryx johni* (Russell). *Zoos' s Print Journal* **22**, 2909–2912 (2007).
50. Price, R. Microdermatoglyphics - An appeal for standardization of morphology and terminology with comments on recent studies of North American natricines. *J. Herpetol.* **24**, 324–325 (1990).
51. Price, R. Dorsal snake scale microdermatoglyphics - Ecological indicator or taxonomic tool? *J. Herpetol.* **16**, 294–306 (1982).
52. Renous, S., Gasc, J. P. & Diop, A. Microstructure of the tegumentary surface of the Squamata (Reptilia) in relation to their spatial position and their locomotion. *Forts. Zool.* **30**, 487–289 (1985).
53. Hazel, J., Stone, M., Grace, M. S. & Tsukruk, V. V. Nanoscale design of snake skin for reptation locomotions via friction anisotropy. *J. Biomech.* **32**, 477–484 (1999).
54. Berthé, R. A., Westhoff, G., Bleckmann, H. & Gorb, S. N. Surface structure and frictional properties of the skin of the Amazon tree boa *Corallus hortulanus* (Squamata, Boidae). *J. Comp. Physiol. A* **195**, 311–318 (2009).
55. Klein, M. C., Deuschle, J. K. & Gorb, S. N. Material properties of the skin of the Kenyan sand boa *Gongylophis colubrinus* (Squamata, Boidae). *J. Comp. Physiol. A* **196**, 659–668 (2010).
56. Oren, M. & Nayar, S. K. Generalization of Lambert's reflectance model. *SIGGRAPH*. **94**, 239–246 (1994).
57. Joger, U. & Courage, K. Are palaearctic "rattlesnakes" (*Echis* and *Cerastes*) monophyletic? *Kaupia* **8**, 65–81 (1999).
58. Hecht, E. *Optics* (Addison Wesley, 2002).
59. Roth, S. I. & Jones, W. A. The ultrastructure and enzymatic activity of the boa constrictor (*Constrictor constrictor*) skin during the resting phase. *J. Ultrastruct. Res.* **18**, 304–323 (1967).
60. Maderson, P. F. A., Rabinovitz, T., Tandler, B. & Alibardi, L. Ultrastructural contributions to an understanding of the cellular mechanisms in lizard skin shedding with comments on the function and evolution of a unique lepidosaurian phenomenon. *J. Morphol.* **236**, 1–24 (1998).
61. Land, M. F. The physics and biology of animal reflectors. *Prog. Biophys. Mol. Biol.* **24**, 75–106 (1972).
62. Osorio, D. & Ham, A. D. Spectral reflectance and directional properties of structural coloration in bird plumage. *J. Exp. Biol.* **205**, 2017–2027 (2002).
63. Vukusic, P., Sambles, J. R. & Lawrence, C. R. Structurally assisted blackness in butterfly scales. *Proc. R. Soc. Lond. B* **271**, 237–239 (2004).
64. Lu, R., Koenderink, J. J. & Kappers, A. M. L. Optical properties (bidirectional reflection distribution functions) of velvet. *Appl. Opt.* **37**, 5974–5984 (1998).
65. Knoll, F. Über den Glanz der Blumenblätter. *Photographie und Forschung* **2**, 137–148 (1938).
66. Kugler, H. Blütenökologische Untersuchungen mit Hummeln. X. Die Reizwirkung von Samt und Seidenglanz. *Planta* **32**, 268–285 (1941).
67. Spezzano, V. Reproduction of *Bitis gabonica rhinoceros* (Schlegel, 1855) in captivity. *Literatura serpentium* **6**, 56–65 (1986).
68. Lenk, P., Herrmann, H. W., Joger, U. & Wink, M. Phylogeny and taxonomic subdivision of Bitis (Reptilia: Viperidae) based on molecular evidence. *Kaupia* **8**, 31–38 (1999).
69. Lenk, P., Kalyabina, S., Wink, M. & Joger, U. Evolutionary relationships among the true vipers (Reptilia: Viperidae) inferred from mitochondrial DNA sequences. *Mol. Phylogenet. Evol.* **19**, 94–104 (2001).
70. Broadley, D. G., Doria, C. & Wigge, J. *Snakes of Zambia: an atlas and field guide* (Edition Chimaira, Frankfurt am Main, 2003).
71. Angelici, F. M., Effah, C., Inyang, M. A. & Luiselli, L. A preliminary radiotracking study of movements, activity patterns and habitat use of free-ranging Gaboon vipers, *Bitis gabonica. Revue d'Ecologie (Terre et Vie)* **55**, 45–55 (2000).
72. Marsh, N. A. & Whaler, B. C. Review article: the gaboon viper (*Bitis gabonica*): its biology, venom components and toxinology. *Toxicon* **22**, 669–694 (1984).
73. Brattstrom, B. H. The coral snake "mimic" problem and protective coloration. *Evolution* **9**, 217–219 (1955).
74. Endler, J. A. On the measurement and classification of colour in studies of animal colour patterns. *Biol. J. Linn. Soc.* **41**, 315–352 (1990).
75. Gomez, D. & Théry, M. Influence of ambient light on the evolution of colour signals: comparative analysis of a Neotropical rainforest bird community. *Ecol. Lett.* **7**, 279–284 (2004).
76. Salisbury, F. B. Twilight Effect: Initiating dark measurement in photoperiodism of *Xanthium*. *Plant. Physiol.* **67**, 1230–1238 (1981).
77. Endler, J. A. The color of light in forests and its implications. *Ecol. Monogr.* **63**, 1–27 (1993).
78. Tercafs, R. R. Transmission of ultra-violet, visible and infra-red radiation through the keratinous layer of reptile skin (Serpentes and Sauria). *Ecology* **44**, 214–218 (1963).
79. Norris, K. S. The evolution and systematics of the iguanid genus *Uma* and its relation to the evolution of other North American desert reptiles. *B. Am. Mus. Nat. Hist.* **114**, 251–326 (1958).
80. Hutchinson, V. H. & Larimer, J. L. Reflectivity of the integuments of some lizards from different habitats. *Ecology* **41**, 199–209 (1960).
81. Pughe, C. E. The science of black. *Engineering and Technology* **3**, 20–23 (2008).
82. Brown, R. J. C., Brewer, P. J. & Milton, M. J. T. The physical and chemical properties of electroless nickel–phosphorus alloys and low reflectance nickel–phosphorus black surfaces. *J. Mater. Chem.* **12**, 2749–2754 (2002).
83. Yang, Z. P., Ci, L., Bur, J. A., Lin, S. Y. & Ajayan, P. M. Experimental observation of an extremely dark material made by a low-density nanotube array. *Nano. Lett.* **8**, 446–451 (2008).
84. Srinivasan, C. The blackest black material from carbon nanotubes. *Curr. Sci. India* **94**, 974–975 (2008).
85. Mizuno, K. *et al.* A black body absorber from vertically aligned single-walled carbon nanotubes. *PNAS* **106**, 6044–6047 (2009).
86. Lehman, J. & Sanders, A. Very black infrared detector from vertically aligned carbon nanotubes and electric-field poling of lithium tantalate. *Nano Lett.* **10**, 3261–3266 (2010).
87. Dai, Y. A. *et al.* Subwavelength Si nanowire arrays for self-cleaning antireflection coatings. *J. Mater. Chem.* **20**, 10924–10930 (2010).
88. Iyengar, V. V., Nayak, B. K. & Gupta, M. C. Ultralow reflectance metal surfaces by ultrafast laser texturing. *Appl. Opt.* **49**, 5983–5988 (2010).
89. Saarikoski, I., Suvanto, M. & Pakkanen, T. A. Nanoporous anodized aluminum oxide-coated polycarbonate surface: Tailoring of transmittance and reflection properties. *Thin Solid Films* **516**, 8278–8281 (2008).
90. Ludwig, A. & Webb, K. J. Dark materials based on graphene sheet stacks. *Opt. Lett.* **36**, 106–107 (2011).


## Acknowledgements

We thank Prof. Dr. Horst Bleckmann (Rheinische Friedrich-Wilhelms-Universität Bonn, Institut für Zoologie, Bonn, Germany), Prof. Dr. Helmut Schmitz (Rheinische Friedrich-Wilhelms-Universität Bonn, Institut für Zoologie, Bonn, Germany) and Frank Weinsheimer for supporting this study with advises and material. This work was partially supported by the German Science Foundation (DFG Graduiertenkolleg Bionik, GRK 1572) and by the Federal Ministry of Education, Science and Technology, Germany (BMBF project Biona 01RB0812) to SNG and GW.

## Author contributions

The first and corresponding author M. Spinner discovered and described the anti-reflective structure based effect, conducted the experiments and wrote the main part of the manuscript. The second author A. Kovalev was the advisor for the optical measurements and assisted in the statistical analysis of the data. A. Kovalev and the third author S.N. Gorb were also involved in the interpretation of the results. The last author G. Westhoff contributed to the discussion of ecological importance of the results and was the founder of this project. All authors reviewed the manuscript.

## Additional information

**Competing financial interests:** The authors declare no competing financial interests.



**How to cite this article:** Spinner, M., Kovalev, A., Gorb, S.N. & Westhoff, G. Snake velvet black: Hierarchical micro- and nanostructure enhances dark colouration in *Bitis rhinoceros*. *Sci. Rep.* **3**, 1846; DOI:10.1038/srep01846 (2013).